Concentration and power dependences of level population of 2.8 - μm laser transition in YLF : Er crystals under CW laser diode pumping

A. M. Tkachuk[1], I. K. Razumova[1], A. A. Mirzaeva[2], G. E. Novikov[2], O. A. Orlov[2], A. V. Malyshev[3], and V. P. Gapontsev[4]

[1] Federal Research Center "Vavilov State Optical Institute", St. Petersburg, 199034 Russia, E-mail: tkachuk@mail.rcom.ru,
[2] Institute for Laser Physics, St. Petersburg, 199034 Russia,
[3] A. I. Ioffe Physical-Technical Institute, St. Petersburg, 194121 Russia,
[4]IPG-Laser, GmbH, Siemensstrasse, 7, D-57299 Burbach, E-mail: valentingapontsev@compuserve.com

ABSTRACT

An influence of interionic cross relaxation processes (upconversion, selfquenching) on concentration and power dependences of the inverse population of $^4I_{11/2}$ and $^4I_{13/2}$ laser levels in YLF:Er crystals under CW laser-diode pumping were studied both theoretically and experimentally. Computer simulations were carried out taking into account not only pair interaction but also the multi-ion interaction in the whole system. Optimal Er concentration for 3 - μm CW lasing was estimated as 10 – 15%.

Keywords: crystal, doped ion, rare earth, energy transfer, population.

1. INTRODUCTION

YLF: Er^{3+} crystals are well-known laser media generating in the VIS and IR under selective laser-diode pumping. Possibility for obtaining the inverse population of working levels of laser transitions strongly depends on macrorates of the interionic coupling processes, since just these processes define the working levels' population. Role of interionic coupling sharply increases with dopant concentration.

We report results of theoretical and experimental studies of formation of the inverse population of the working $^4I_{11/2}$ and $^4I_{13/2}$ levels of a 3-μm laser transition in $LiY_{1-x}Er_xF_4$ (x=0.003 ÷1) under CW laser-diode pumping. Mechanisms of the interionic interaction processes and the concentration and pump power density dependences of their macrorates are obtained.

2. EXPERIMENTAL METHODS

Series of 11 samples of $LiY_{1-x}Er_xF_4$ crystals with dopant concentration 0.3 – 100 at.% were studied. Crystals were grown by modified Bridgman – Stockbarger technique.

Experimental dependences of population of the studied levels on erbium concentration were obtained from the intensity of the steady-state luminescence in spectral ranges of transitions from $^4I_{11/2}$ (0.9 – 1μm and 2.7 – 2.9 μm) and $^4I_{13/2}$ (1.4 – 1.6 μm) levels under selective laser-diode pumping in $^4I_{11/2}$. state. Spectra were recorded with a MDR-23 monochromator with computer control. Selective excitation of the $^4I_{11/2}$ level was performed by emission of a DL – 5M module of five InGaAs laser diodes (LD) summed in a fiber with a 230 μm core diameter. The laser diodes emitted radiation in the λ =966-982 nm range which matched the YLF:Er^{3+} absorption was focused on the face of the YLF:Er^{3+} crystals by lens. Output power of the DL-5M module varied within 0÷5 W

Computer simulations were carried out for the spectroscopic model involving 5 lower excited states of erbium ions taking into account the multi-ion interaction in the whole system. A system of rate equations for populations of the excited levels of erbium ions was solved and the population dependences on the dopant concentration and pump power density were derived. For all principal energy-transfer processes, such parameters as radiative and non-radiative

Laser Optics 2000: Solid State Lasers, Vladimir I. Ustugov, Editor,
Proceedings of SPIE Vol. 4350 (2001) © 2001 SPIE · 0277-786X/01/$15.00

probabilities, life-time of excited levels, luminescence selfquenching and upconversion rates were determined from the independent experimental results and theoretical estimations within the framework of known energy transfer theory.

3. RESULTS AND DISCUSSION

Theoretical concentration dependences of steady-state populations of $^4I_{11/2}$ and $^4I_{13/2}$ erbium levels under different pumping power densities were obtained from the system of rate balance equations for the six lowest levels of erbium ion with allowance for intracenter relaxation and inter-ionic coupling processes, such as luminescence self-quenching and up-conversion. All processes involved into calculations under IR LD excitation of YLF: Er^{3+} crystals are indicated by arrows in the energy level scheme in Fig. 1.

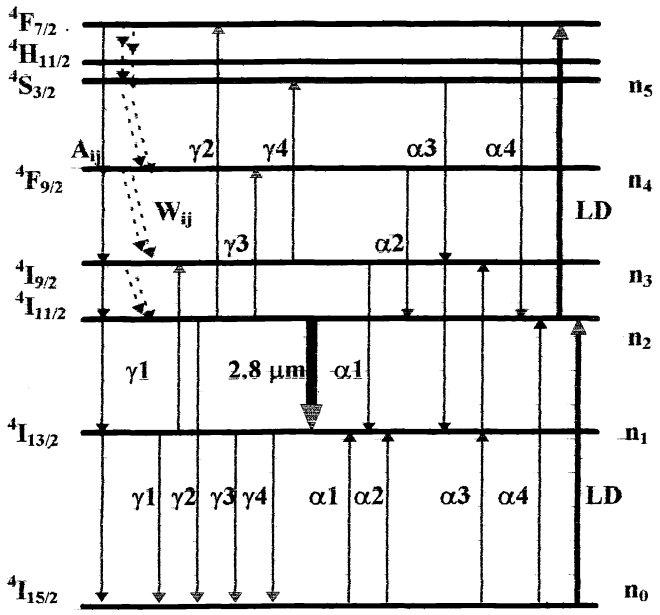

Fig. 1. Energy levels and schemes of radiationless Er-Er coupling in YLF:Er^{3+}. A_{ij} - rediative $i \rightarrow j$ transition probabilities, W_{ij} - radiationless relaxation, α_i - self-quenching and γ_i - upconversion processes. Bold arrow – laser transition.

Table 1. Probabilities of intacenter transitions A_{ij}, W_{ij} and τ_{exp}^{-1} in YLF: Er^{3+} [5].

$n_i \rightarrow n_j$	A_{ij}, c^{-1}	τ_{exp}^{-1}, c^{-1}	W_{ij}, c^{-1}
$1 \rightarrow 0$	129	90	0
$2 \rightarrow 0$	143	250	
$2 \rightarrow 1$	17		0
$3 \rightarrow 0$	19		
$3 \rightarrow 1$	50	$1.5 \cdot 10^{5*}$	
$3 \rightarrow 2$	10		$6.9 \cdot 10^4$
$4 \rightarrow 0$	745		
$4 \rightarrow 1$	31	$3.3 \cdot 10^4$	
$4 \rightarrow 2$	66		
$4 \rightarrow 3$	1.0		$3.2 \cdot 10^4$
$5 \rightarrow 0$	1375		
$5 \rightarrow 1$	567		
$5 \rightarrow 2$	43	$2.5 \cdot 10^3$	
$5 \rightarrow 3$	56		
$5 \rightarrow 4$	10		$2.2 \cdot 10^3$

*) the value of τ_{exp} is from [6].

The system of rate balance equations for normalized populations of erbium levels $n_i = n_i(\mathrm{Er})/n(\mathrm{Er})$, where $n(\mathrm{Er})$ is the relative concentration of Er^{3+} ion $n(\mathrm{Er}) = N_{Er}/N_Y$ was written as follows:

$$dn_1/dt = -A_{10}n_1 + \sum_{i=2}^{5} A_{i1}n_i + 2\alpha_1 n_0 n_3 + \alpha_2 n_0 n_4 + \alpha_3 n_0 n_5 - 2\gamma_1 (n_1)^2 - \gamma_3 n_1 n_2 - \gamma_4 n_1 n_3 = 0$$

$$dn_2/dt = -\sum_{j=0}^{1} A_{2j}n_2 + \sum_{i=3}^{5} A_{i2}n_i + W_{32}n_3 + \alpha_2 n_0 n_4 + 2\alpha_4 n_0 n_5 - 2\gamma_2 (n_2)^2 - \gamma_3 n_1 n_2 + R_{02}n_0 - R_{25}n_2 = 0$$

$$dn_3/dt = -\sum_{j=0}^{2} A_{3j}n_3 - W_{32}n_3 + \sum_{i=4}^{5} A_{i3}n_i + W_{43}n_4 - \alpha_1 n_0 n_3 + \alpha_3 n_0 n_5 + \gamma_1 (n_1)^2 - \gamma_4 n_1 n_3 = 0$$

$$dn_4/dt = -\sum_{j=0}^{3} A_{4j}n_4 + (A_{54} + W_{54})n_5 - \alpha_2 n_0 n_4 + \gamma_3 n_1 n_2 = 0$$

$$dn_5/dt = -\sum_{j=0}^{4} A_{5j}n_5 - W_{54}n_5 - (\alpha_3 + \alpha_4)n_0 n_5 + \gamma_2 (n_2)^2 + \gamma_4 n_1 n_3 + R_{25}n_2 = 0$$

$$dn_0/dt = \sum_{i=1}^{5} A_{i0}n_0 - \alpha_1 n_0 n_3 - \alpha_2 n_0 n_4 - (\alpha_3 + \alpha_4)n_0 n_5 + \gamma_1 (n_1)^2 + \gamma_2 (n_2)^2 + \gamma_3 n_1 n_2 + \gamma_4 n_1 n_3 - R_{02}n_0 = 0,$$

where A_{ij} [c^{-1}] are the probabilities of radiative transitions from "i" to "j" levels; W_{ij} [c^{-1}] are the probabilities of non-radiative multiphonon transitions; parameters α_i (i = 1 - 4) are the macrorates for self-quenching processes (Er – Er self-quenching), parameters γ_j (j = 1 - 4) are the macrorates of up-conversion processes (up-conversion Er – Er) for the cross-relaxation schemes indicated by arrows in Fig. 1.

Parameters of radiative and non-radiative relaxations for $LiY_{1-x}Er_xF_4$ (x=0.003-1) reported in [5-6] and the values of A_{ij} , W_{ij}, and lifetimes of excited levels measured for low-concentrated samples (x = 0.5%) are given in the Table 1.

Energy transfer microparameters of migration C_{DD} (Table 2) and selfquenching C_{DA} (Table 3) were obtained by the model quantum-mechanical calculation in [1-4]. The energy level diagram in Fig. 1 shows schemes of cross-relaxation transitions, for which migration and energy-transfer microparameters were calculated within the framework of electro-static (multupole-multipole) interaction of erbium ions. From the ratio of C_{DD} and C_{DA} microparameters, the transfer mechanisms were determined and macrorates were estimated for the self-quenching and up-conversion processes in framework of jump (J) or static (S) decay models. Good agreement between theoretical and experimental estimates of the energy-transfer macrorates and their concentration dependences calculated in different energy-transfer models [1, 4] enabled us to estimate the effective values of the energy transfer constants α_i and to obtain the analytical form of their concentration dependences, which were substituted into the rate balance equations. Up-conversion constants γ_i were estimated using calculated microparameters and formulas from [1-4].

Table 2. Calculated microparameters of migration (C_{DD}) in YLF-Er^{3+}

Level $n_{i,a}$	Cross-relaxation process, transition $(i \rightarrow j)_a$: $(j \rightarrow i)_b$	$C_{DD}^{dd}.10^{40}$ cm^6s^{-1}	$C_{DD}^{dq}.10^{55}$ cm^8s^{-1}	$C_{DD}^{qq}.10^{69}$ $cm^{10}s^{-1}$
$^4I_{13/2}$	1. $(^4I_{13/2} \rightarrow {}^4I_{15/2})$:$(^4I_{15/2} \rightarrow {}^4I_{13/2})$	24.43	21.04	3.377
$^4I_{11/2}$	2. $(^4I_{11/2} \rightarrow {}^4I_{15/2})$:$(^4I_{15/2} \rightarrow {}^4I_{11/2})$	1.557	8.54	8.725
$^4I_{9/2}$	3. $(^4I_{9/2} \rightarrow {}^4I_{15/2})$:$(^4I_{15/2} \rightarrow {}^4I_{9/2})$	0.167	0	0
$^4F_{9/2}$	4. $(^4F_{9/2} \rightarrow {}^4I_{15/2})$:$(^4I_{15/2} \rightarrow {}^4F_{9/2})$	4.67	0	0
$^4S_{3/2}$	5. $(^4S_{3/2} \rightarrow {}^4I_{15/2})$:$(^4I_{15/2} \rightarrow {}^4S_{3/2})$	1.013	0	0
$^4H_{11/2}$	6. $(^2H_{11/2} \rightarrow {}^4I_{15/2})$:$(^4I_{15/2} \rightarrow {}^2H_{11/2})$	7.31	504	6475
$^4F_{7/2}$	7. $(^4F_{7/2} \rightarrow {}^4I_{15/2})$:$(^4I_{15/2} \rightarrow {}^4F_{7/2})$	11.04	0	0

Table 3. Calculated microparameters of self-quenching and up-conversion (C_{DA}) in YLF-Er^{3+}.

Levels, $n_{i,a}$; $n_{k,b}$	Cross-relaxation process, transition $(i \rightarrow j)_a$: $(k \rightarrow l)_b$	$C_{DA}^{dd}.10^{40}$ cm^6s^{-1}	$C_{DA}^{dq}.10^{55}$ cm^8s^{-1}	$C_{DA}^{qq}.10^{70}$ $cm^{10}s^{-1}$
	Er – Er self-quenching			
$^4I_{9/2}$, $^4I_{15/2}$	1. $(^4I_{9/2} \rightarrow {}^4I_{15/2})$:$(^4I_{15/2} \rightarrow {}^4I_{13/2})$ - hω	0.60	5.44	7.9
$^4F_{9/2}$, $^4I_{15/2}$	2. $(^4F_{9/2} \rightarrow {}^4I_{11/2})$:$(^4I_{15/2} \rightarrow {}^4I_{13/2})$ -2hω	0.019	0.094	0.124
$^4S_{3/2}$, $^4I_{15/2}$	3. $(^4S_{3/2} \rightarrow {}^4I_{9/2})$:$(^4I_{15/2} \rightarrow {}^4I_{13/2})$ - hω	10.83	9.32	0
$^4S_{3/2}$, $^4I_{15/2}$	4. $(^4S_{3/2} \rightarrow {}^4I_{13/2})$:$(^4I_{15/2} \rightarrow {}^4I_{9/2})$ - hω	0.84	0	0
$^2H_{11/2}$, $^4I_{15/2}$	5. $(^2H_{11/2} \rightarrow {}^4I_{9/2})$:$(^4I_{15/2} \rightarrow {}^4I_{13/2})$	38.31	1217	1902
	Er→Er up-conversion			
$^4I_{13/2}$; $^4I_{13/2}$	1. $(^4I_{13/2} \rightarrow {}^4I_{9/2})$:$(^4I_{13/2} \rightarrow {}^4I_{15/2})$ + hω	47	42.2	1.47
$^4I_{11/2}$; $^4I_{11/2}$	2. $(^4I_{11/2} \rightarrow {}^4F_{7/2})$:$(^4I_{11/2} \rightarrow {}^4I_{15/2})$	4.15	30.36	32.11
$^4I_{11/2}$; $^4I_{13/2}$	3. $(^4I_{11/2} \rightarrow {}^4F_{9/2})$:$(^4I_{13/2} \rightarrow {}^4I_{15/2})$ + 2hω	1.39	1.803	0.515
$^4I_{13/2}$; $^4I_{11/2}$	4. $(^4I_{13/2} \rightarrow {}^4F_{9/2})$:$(^4I_{11/2} \rightarrow {}^4I_{15/2})$ + 2hω	0.027	0.24	0.515
$^4I_{9/2}$; $^4I_{13/2}$	5. $(^4I_{9/2} \rightarrow {}^4S_{3/2})$:$(^4I_{13/2} \rightarrow {}^4I_{15/2})$ + hω	27.6	23.77	0
$^4I_{13/2}$; $^4I_{9/2}$	6. $(^4I_{13/2} \rightarrow {}^4S_{3/2})$:$(^4I_{9/2} \rightarrow {}^4I_{15/2})$ + hω	0.61	0	0

The analytical form of concentration dependence of the constants of the luminescence self quenching and up-conversion are listed in Tables 4.

To compare calculated results with the experimental values of luminescence intensity, which represent the integrated signals of excited volume, we had to spatially integrate the calculated $N_i=n_i x N_Y$ magnitude over the excited volume ($N_Y = 1.39 \cdot 10^{22}$ cm $^{-3}$ is the number of substituted yttrium positions per unit volume). Since n_i itself strongly depends on a distance from irradiated crystal surface, numerical integration was carried out for fixed $x = 0.01 \div 1$ values.

Table 4. Analytical form of concentration dependence of the macrorates of the cross-relaxation processes of the luminescence self-quenching (α_i) and up-conversion (γ_i) in YLF: Er^{3+} crystals. Parameters were obtained for the jumping (J) and static (S) models using the calculated values of the transfer microparameters C_{DD} and C_{DA} from [1].

Model	Transition $(i \rightarrow j)_a$: $(k \rightarrow l)_b$	Parameters (α_i, γ_i), s^{-1}
S	$(^4I_{9/2} \rightarrow {}^4I_{15/2})$:$(^4I_{15/2} \rightarrow {}^4I_{13/2})$ -hω	$\alpha_1 = 1.29*10^2x^2 + 3.35*10^2(x^2)^{4/3} + 2.85*10^2(x^2)^{5/3}$
J	$(^4F_{9/2} \rightarrow {}^4I_{11/2})$:$(^4I_{15/2} \rightarrow {}^4I_{13/2})$ -2hω	$\alpha_2 = 1.91*10^2x^2$
S	$(^4S_{3/2} \rightarrow {}^4I_{9/2,\ 13/2})$:$(^4I_{15/2} \rightarrow {}^4I_{13/2,9/2})$-hω	$\alpha_3 = 2.5*10^3x^2 + 5.75*10^2(x^2)^{4/3}$
J	$(^2H_{11/2} \rightarrow {}^4I_{9/2})$:$(^4I_{15/2} \rightarrow {}^4I_{13/2})$	$\alpha_4 = 5.4*10^3x^2$
J	$(^4I_{13/2} \rightarrow {}^4I_{9/2})$:$(^4I_{13/2} \rightarrow {}^4I_{15/2})$ +hω	$\gamma_1 = 2.26*10^4 (n_1 \cdot x)^2$
S	$(^4I_{11/2} \rightarrow {}^4F_{7/2})$:$(^4I_{11/2} \rightarrow {}^4I_{15/2})$	$\gamma_2 = 8.9*10^2 (n_2 \cdot x)^2 + 3.35*10^2(n_2 \cdot x)^{8/3} + 2.85*10^2(n_2 \cdot x)^{10/3}$
J	$(^4I_{11/2} \rightarrow {}^4F_{9/2})$:$(^4I_{13/2} \rightarrow {}^4I_{15/2})$ +2hω	$\gamma_3 = 1.0*10^3(n_1 \cdot x)(n_2 \cdot x)$
J	$(^4I_{9/2} \rightarrow {}^4S_{3/2})$:$(^4I_{13/2} \rightarrow {}^4I_{15/2})$ +hω	$\gamma_4 = 1.0*10^3(n_1 \cdot x)(n_3 \cdot x)$

Excited volume was divided into layers, where n_i was assumed to be constant. For a fixed layer within excited volume located at the distance r from the sample surface, the pump power density P is determined by the Bouguer law: $P(r) = P_0 \exp(-\Sigma \sigma_{ij} n_i x N_Y r)$, where P_0 is the incident power density, $x = N_{Er}/N_Y$ is the relative concentration of dopant ions. $R_{ij} = \sigma_{ij} P/p_0$ are the rates of absorption transitions under the pumping radiation with the photon energy $p_0 = hc/\lambda_p$. According to the spectral composition of the emission of the LD-module, absorption can only occur from the ground $^4I_{15/2}$ and the second excited $^4I_{11/2}$. states. Absorption cross-section σ_{02} for the ground $^4I_{15/2}$ state was obtained from the experimental absorption spectra [5] and σ_{25} – absorption from $^4I_{11/2}$ state was taken from the excited state absorption spectrum [7].

Theoretical dependences of the steady-state populations of $^4I_{11/2}$ and $^4I_{13/2}$ levels on relative erbium concentration $x = 0 - 1$ were calculated for the pump power densities used in experiments $P = 127$, 223, 318, and 395 kW/cm^2 (LD emission with the incident power, respectively, 1, 1.75, 2, and 3 W focused in a spot with 1 mm diameter).

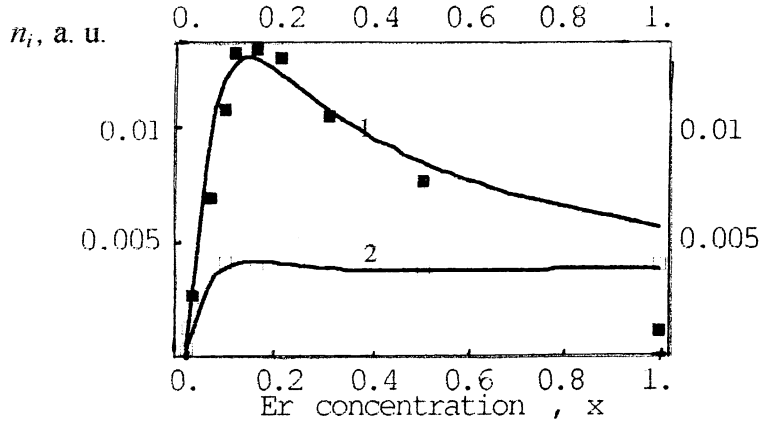

Fig. 2. Calculated (solid curves) and experimental (squares) concentration dependences of relative populations $N_i/N_Y = n_i x$ of the $^4I_{11/2}$ (curve 1) and $^4I_{13/2}$ (curve 2) working levels of 3μm laser transition on the Er concentration x under CW LD pumping in $LiY_{1-x}Er_xF_4$:Er crystals. Pump power density $R_{02} = 100$ W·cm^{-2}, T=300°K.

Experimental concentration dependences of populations of $^4I_{11/2}$ and $^4I_{13/2}$ erbium levels in YLF:Er^{3+} crystals with x=0.003 ÷1 were obtained from the luminescence spectra recorded at the same pump power densities. Under CW pumping, relative population of $^4I_{11/2}$ increases with erbium concentration up to the maximum in the region $N_{Er} \approx 10 \div 15$ at% and decreases for $N_{Er} > 20$ at%. Relative population of $^4I_{13/2}$ level increases with erbium concentration to ≈ 10 at% and remains constant within the range of high erbium concentration up to $N_{Er} > 50$ at%. Comparison of the calculated and experimental results are given in Fig. 2.

Experimental dependences of relative population of the $^4I_{11/2}$ and $^4I_{13/2}$ working levels of 3μm transition on the pump power density were measured for all 11 samples with different erbium concentrations for pump power densities 57, 100, 141, and 175 W/cm^{-1} cm^2 (LD emission with, respectively, 1, 1.75, 2, and 3 W – incident power focused in a spot with 1.5 mm diameter).

Fig. 3 shows experimental and theoretical data for the erbium concentration x = 0.15 (N_0=15 at. %).

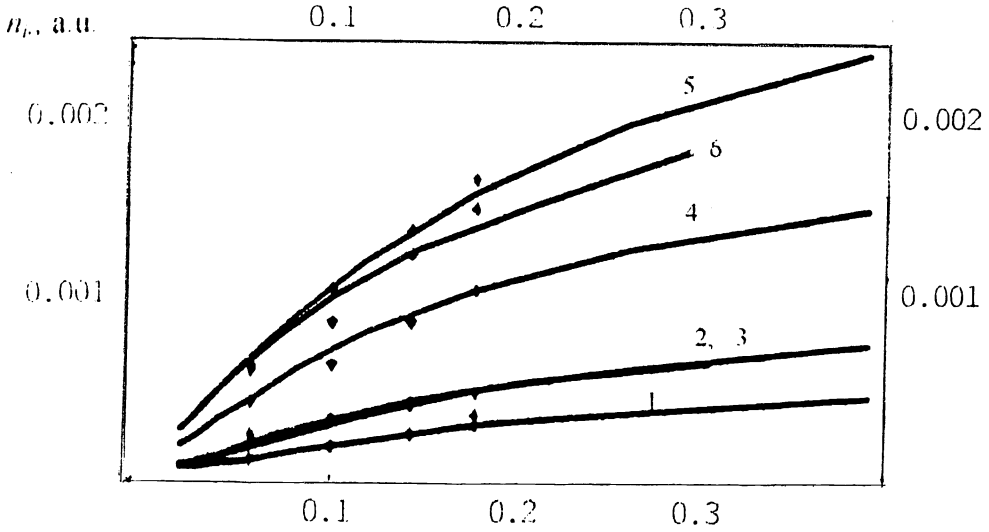

Fig. 3. Calculated (solid curves) and experimental (points) dependences of relative populations $N_i/N_Y=n_ix$ of the $^4I_{13/2}$ (curves 1 - 3) and $^4I_{11/2}$ (curves 4 - 6) erbium levels on pump power density R_{02} in kW·cm^{-2} under CW LD pumping in $LiY_{1-x}Er_xF_4$:Er crystals. The Er concentration x = 0.05 (curves 1, 4), 0.15 (curves 2, 5) and 0.3 (curves 3, 6), T=300°K.

Obtained theoretical results are in a good agreement with presented experimental data and also with results reported on experimental studies of the concentration dependence of the efficiency of 3μm lasing in YLF:Er^{3+} on the $^4I_{11/2} \rightarrow {}^4I_{13/2}$ transition under CW pumping of $^4I_{11/2}$ level [8-10]. The maximal slope efficiency of YLF:Er laser η_{sl}=50% was obtained in crystals with erbium concentration N_{Er} =15 ат.% [8]. Noteworthy is that, in contrast with the data reported e. g. in [8], the theoretical model used in our work does not involve any fitting parameters. Therefore, one can conclude that the set of parameters used in our calculations for the intracenter radiative and non-radiative probabilities and the estimated macrorates of the inter-center energy transfer processes (selfquenching and upconversion) obtained by the model quantum-mechanical calculation could be further employed for estimation of the output characteristics of 2.8 μm YLF:Er^{3+} CW lasers and optimization of the composition of their active elements.

4. CONCLUSION

Theoretical calculations with the energy transfer constants of self-quenching and up-conversion obtained by the method of model quantum-mechanical calculation show good agreement with experimental results. One can conclude that population of the working levels of 3-μm laser transition in $LiY_{1-x}Er_xF_4$ (x=0.003 ÷1) can be reliably described with the rate balance equations allowing for the non-linear energy transfer processes with theoretically estimated transition probabilities and energy transfer rates.

Thus, proposed spectroscopic model of YLF:Er^{3+} crystals without any fitting parameters reliably describes experimental concentration and power dependences of the steady-state population of the erbium levels, and can be used for prediction of the laser properties of studied crystals.

5. ACKNOWLEDGMENTS

The work was partly supported by INTAS, Grant No INTAS-97-787, and Russian Foundation for Basic Researches, Grants No 98-02-18102 and 00-02-16637

6. REFERENCES

1 Tkachuk A M , Klokishner S I , and Petrov M V *Opt. Spectrosc.* (USSR) **59**, (4), pp 485-491, 1986 [*Opt Spektrosk* Vol 59, No 4, pp 802-811, 1985]
2 Klokishner S I , and Tkachuk A M *Opt. Spektrosk* **68**, (4), pp 745-752, 1990
3 Tkachuk A M , Klokishner S I *Opt. Spectrosc. (USSR),* **61**, (1), pp 55-61, 1986 [*Opt Spektrosk* **61**, (1), pp 84-90, 1986]
4 Tkachuk A M *Opt. Spectrosc (USSR),* **68**, (6), pp 775-783, 1990 [1990 *Opt. Spektrosk* **68**, (6), pp 1324-1336, 1990]
5 Tkachuk A M , Poletimova A V , andPetrov M V *Opt. Spectrosk.* **59**, (5), pp 1136-1139, 1985
6 Li C , Guyot Y , Linares C , Moncorge R , and Joubert M -F *OSA Pros. of Advansed Solid State Lasers.* **15**, pp 91-95 1993
7 Labbe Ch *Theses, University of Caen, France* 1999
8 Tikerpae M , Jackson S D , and King T A *J. of Modern Optics* **45**, (6), pp 1269-1284 1998
9 Pollnau M , Luthy W , Weber H P , Jensen T , Huber G , Cassanho A , Jenssen H P , McFarline R A *Opt. Lett* **21**, (1), pp 48-50 1996
10 Wyss Chr , Luthy W , Weber H P , Rogin P , Hulliger J *Opt Commun.* **139,** pp 215-218, 1997